JOURNAL OF SCIENCE TECHNOLOGY AND EDUCATION 9(2), JUNE, 2021
ISSN: 2277-0011; Journal homepage: www.atbuftejoste.com

Trajectory Analysis and Dynamic Simulation of a 6 DOF Industrial Manipulator

[1]Abubakar Umar, [1]Zhanqun Shi*, Wei Wang, Zulfiqar Ibrahim Bibi Farouk
[1]*Department of Mechanical Engineering,*
Hebei University of Technology,
Tianjin – China
[2]*Department of Mechanical Engineering,*
Tianjin University,
Tianjin – China

ABSTRACT
The popularization of the articulate industrial manipulator in most industrial work spaces is majorly as a result of its dexterity, robustness, and its ability to reach difficult configurations during an industrial task. This has inspired the research into the design and analysis of an articulate industrial manipulator to improve its accuracy and agility. The manipulator was modelled, then its kinematic and dynamic properties were established in Siemen's Unigraphics software. An algorithm that generates and analyses the trajectory is presented, the trajectory was first parametrically defined, then dynamics of the manipulator was evaluated using Newton-Euler formulations to derive a state-space dynamic model which is a function of only the joints position (i.e. the only input required is the joints position) which can be easily updated as it moves along the desired path, the results were compared with results obtained from ADAMS and was seen to be more efficient. The algorithm was then implemented on the proposed manipulator and simulated in MATLAB by first setting it to force-free conditions, then it was loaded with 5kg and 10kg exerting a maximum torque of 5N and 10N respectively at the end-effector and simulated again. The algorithm was found to be computationally efficient and practical, furthermore the algorithm would help students and researchers alike to analyze the trajectories and dynamics for manipulators more efficiently thereby enabling them to implement more stable control strategies for industrial manipulator.

ARTICLE INFO
Article History
Received: February, 2020
Received in revised form: March, 2021
Accepted: May, 2021
Published online: June, 2021

KEYWORDS
Robot, manipulator; trajectory; dynamics; simulation; analysis.

INTRODUCTION

A robot is a programmable machine capable of carrying out complex series of actions automatically. Robots can be categorized into autonomous (unmanned) vehicles or industrial manipulators. An industrial manipulator is a device used to manipulate objects without direct human contact. An industrial manipulator consists of a combination of links and joints. The links are solid members connecting joints while the joints are moveable parts that cause motion between adjacent links.

A 6 Degree-of-Freedom (DOF) articulate manipulator is modelled with the basic characteristics of a human arm. Degree of freedom (DOF) refers to the number of independent coordinates that fully describes the robot's configuration [3], or simply the number of joints in the robot. The first three joints represent the waist, shoulder and elbow of a human arm, they can be controlled to reach any specified position within its work-space giving the manipulator desired pose. The human wrist is a spherical joint, which is an Omni-directional joint capable of orienting (pointing) the manipulator in any direction even when other joints are stagnant. In reality, spherical joints can neither be controlled by electrical, pneumatic nor hydraulic actuators making it difficult

Corresponding author: Zhanqun Shi, Wei Wang ✉ *z_shi@hebut.edu.cn ✉ *Department of Mechanical Engineering, Hebei University of Technology, Tianjin - China.*

to implement in robots. For this purpose, three joints are implemented with a roll-pitch-roll configuration to depict the spherical joint of a human wrist. The first three joints can therefore be said to position the robot manipulator, while the last three joints orient the robot manipulator. All six joints of the robot manipulator can be controlled to produce the desired motion of the robot end-effector (tool) along the desired trajectory (path). The robot end-effector could be a welding gun, a cutting/grinding disc, camera or even a laser pen. The act of following a desired trajectory as closely as possible is called trajectory tracking. The quality of a robot control scheme is determined by its trajectory tracking efficiency.

REVIEW OF LITERATURE

Compilation of a robot dynamics algorithm for robot motion control is centered on deriving of joint actuating forces and torques which produce the required motion of the end-effector. The two most-widely implemented robot motion control schemes are the model-based and the non-model- based control schemes. Comparative analysis [1] showed that the model-based controller gives a better trajectory tracking performance while the later was found to be more robust. The model-based algorithm requires the exact knowledge of the robot's dynamic parameters but in reality it is impossible to determine the exact physical parameter of any part. As the uncertainties in the dynamic parameter model increases, the performance of the controller sharply deteriorates.

The conventional Proportional-Integral-Derivative (PID) controller is a non-model-based controller, it does not require computation of the robot dynamic model but lacks the accuracy required by high speed/precision and heavy load robots [2] this led to the development of the more advanced computed-torque control methods [3], [4], [5] & [6] based on the complete dynamic model of the robot. Reference [7] Presented a controller based on complete dynamic torque algorithm which derives the inverse dynamic model of the robot using trajectory pattern method. The motion path is parameterized (divided) into several small time periods (segments), along which the motion is described by a specific trajectory pattern. The actuating force and torque between every segment is derived using the position, velocity and acceleration values within the segment and also the dynamic parameters of the robot. This remains the most popular robot control scheme which forms the basis for most advanced robot control schemes being used to date. Over the years, the computed-torque controller [8], the Augmented Proportional-Derivative (PD) controller [9] and the impedance controller [10] have been successfully used in a wide range of robot applications.

Adaptive control schemes have been shown to be capable of combining both the efficiency of the model-based algorithm and the robustness of the no-model-based algorithm. Reference [11] presented an algorithm that estimates the kinematic and dynamic parameters of a robot without necessarily knowing the structure of the robot at force-free conditions (no load). Link-by-Link (Starting from the end-effector link), a series of known inputs (actuating forces/torque) are introduced while the outputs (robot position, velocity and acceleration) are measured by sensors. The Newton-Euler formulation was modified so that it becomes linear in the dynamic parameters then an error model was introduced. Parameter identification was achieved using the least-square optimization algorithm based on this modified Newton-Euler formulation. A similar algorithm was presented in [12] for dynamic parameter identification of robot manipulators powered by servo motors by taking the characteristics of the servo unit into consideration. The sensors acquired Data at impulse-excited trajectories which introduced noise in the sensor's readings. Periodic-excited trajectories was proposed in [13] based on Modified Fourier-Series. Reference [14] used the Power model for dynamic parameter identification to increase the computational efficiency of the algorithm, against the alternative inverse dynamic model. Yet all these algorithms were implemented on a link-by-link approach which therefore requires a reasonably large computation time. In [2] the computational time was reduced by identifying all the dynamic parameters of the robot in only two instances, at the wrist and elbow joints (i.e. three joints at a time). Considering that in some robots, the three joints are coincident at these joints (the wrist and elbow) and appreciating the large difference in the inertia parameters between the

*Corresponding author: Zhanqun Shi, Wei Wang ✉ *z_shi@hebut.edu.cn ✉ Department of Mechanical Engineering, Hebei University of Technology, Tianjin - China.

wrist and the elbow joints especially in force-free conditions, the effectiveness of this method over the link-by-link approach was demonstrated. Most documented works on robot dynamic parameter identification focused on the estimation veracity, [15] focused on the convergence speed of the algorithm. Slow convergence and long training time has hindered the practical application of Adaptive control schemes in robotics.

Despite recent improvements in dynamic algorithms for robot motion control, some manufacturers, students and researchers are observed to still use general purpose commercial software [16][17] or implement conventional PID controller without necessarily considering the trajectory or dynamics, this is assumed to be as a result of the complex nature of these algorithms. The conventional PID fails to characterize the complex, highly coupled and non-linear second-order differential equation that defines the joint dynamics. This often result in oscillations or overshoot of the end effector [2][18]. A customized algorithm has been found to compute the inverse dynamics of robot manipulators over 3.4 times faster than the most efficient general purpose algorithm [6][19],[20]. A simplified algorithm is hereby presented for computed-torque dynamic analysis and simulation. The algorithm would show a step-by-step approach of computing the robot trajectory given the initial and final robot configuration, then it would go further to develop a dynamic model for the robot and the results simulated in MATLAB.

The links of the proposed manipulator were modelled with 10mm aluminum plates and steel bearings, while the joints are to be powered by servo-motors. The total reach of the manipulator is 1000mm with a total mass of 15.6kg. The link lengths a, offset lengths d, joint angles θ and offset angle γ of the proposed manipulator are presented in Table 1 below as prescribed by Danavit-Hatenberg (D-H). In Figure 1, the first joint is coincident with the centroid axis of the base (i.e. the global y-axis), therefore it can be said to revolve about its own axis. The fourth and sixth joints also revolve about their own centroid axis while the second, third and fifth joints are perpendicular to the centroid axis (i.e. along the global z-axis). Observe that the later joints are parallel to each other, and if the robot is outstretched vertically to a singular configuration, the former joints would be seen to be coincidental.

Table 1: D-H Parameters

s/n	a (mm)	d (mm)	θ	γ
Joint 1	130	0	variable	π/2
Joint 2	385	0	variable	0
Joint 3	115	0	variable	π/2
Joint 4	0	271	variable	- π/2
Joint 5	0	0	variable	π/2
Joint 6	0	97	variable	0

TRAJECTORY ANANLYSIS

The trajectory problem of an industrial manipulator requires that the path of the end-effector of the manipulator should be mathematically described. If the manipulator is to travel from a point 'A' along a given path to a point 'B' within a given time frame, the position and orientation of the manipulator along that path must be parameterized and completely defined.

End-Effector Position Analysis

Let 'P' be the path of travel of the end-effector, then the initial and final positions (P_i and P_f) in Cartesian space would be

$$P_i = \begin{vmatrix} p_{xi} \\ p_{yi} \\ p_{zi} \end{vmatrix} \quad \text{and,} \tag{1}$$

$$P_f = \begin{vmatrix} p_{xf} \\ p_{yf} \\ p_{zf} \end{vmatrix} \quad \text{Therefore,} \tag{2}$$

*Corresponding author: Zhanqun Shi, Wei Wang ✉ *z_shi@hebut.edu.cn ✉ Department of Mechanical Engineering, Hebei University of Technology, Tianjin - China.

JOURNAL OF SCIENCE TECHNOLOGY AND EDUCATION 9(2), JUNE, 2021
ISSN: 2277-0011; Journal homepage: www.atbuftejoste.com

$$P = |P_i \quad P_f| = \begin{vmatrix} p_{xi} & p_{xf} \\ p_{yi} & p_{yf} \\ p_{zi} & p_{zf} \end{vmatrix} \qquad (3)$$

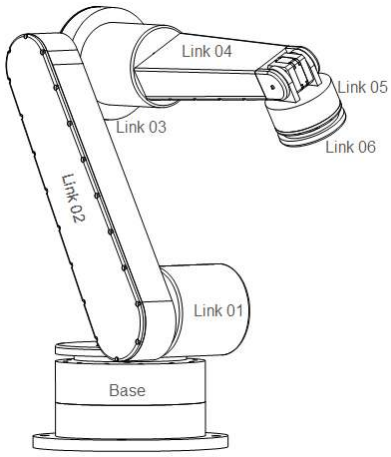

Figure 1. Model of a 6 DOF Industrial Manipulator

The end-effector starts at position P_i at an initial time zero to the final position P_f at a final time t. The polynomial solution of the trajectory problem usually results in a trapezoidal velocity profile with three visible segments (i.e. the acceleration, constant velocity and deceleration segments), but if the path is short, the aim of an industrial process is usually to optimize time therefore the polynomial solution would result in a parabolic or triangular velocity profile with only an acceleration and deceleration segment, with the constant velocity profile is completely omitted. Let t_c represent the time halfway across the path which signifies the end of the acceleration segment and at the beginning of the deceleration segment, therefore;

$$\left.\begin{array}{l} t_i = 0 \\ t_c = t/2, \ and \\ t_f = t \end{array}\right\} \qquad (4)$$

From the equation of a straight line;

$$\left.\begin{array}{l} P_i = at_i + b \\ P_f = at_f + b \end{array}\right\} \qquad (5)$$

Solving the equation (5) above, the values of the constants a and b can be evaluated and used to determine the point P_c which corresponds to the time t_c at the end of acceleration segment and the beginning of the deceleration segment as follows;

$$P_c = at_c + b \qquad (6)$$

Therefore the end-effector velocity and acceleration can be deduced as follows;

$$\dot{\theta}_c = (P_c - P_i)/t_c \qquad (7)$$

$$\ddot{\theta}_c = \dot{\theta}_c/t_c \qquad (8)$$

End-Effector Orientation

If the initial and final orientation (Q_i and Q_f) are known, then a single rotation matrix 'Q' which represents the transformation of the end-effector in Cartesian space would be;

$$|Q| = |Q_i^T| * |Q_f| = \begin{vmatrix} q_{11} & q_{12} & q_{13} \\ q_{21} & q_{22} & q_{23} \\ q_{31} & q_{32} & q_{33} \end{vmatrix} . \qquad (9)$$

The single axis rotation method can be used to determine the magnitude and direction of rotation as shown below then (7) and (8) can be used to determine the rate of change of the robot's orientation from α(0) to α(t).

$$\alpha = cos^{-1}\left(\frac{q_{11}+q_{22}+q_{33}-1}{2}\right) . \qquad (10)$$

$$|e| = \frac{1}{2sin\alpha}\begin{vmatrix} q_{32} - q_{23} \\ q_{13} - q_{31} \\ q_{21} - q_{12} \end{vmatrix} . \qquad (11)$$

*Corresponding author: Zhanqun Shi, Wei Wang ✉ *z_shi@hebut.edu.cn ✉ Department of Mechanical Engineering, Hebei University of Technology, Tianjin - China.

JOURNAL OF SCIENCE TECHNOLOGY AND EDUCATION 9(2), JUNE, 2021
ISSN: 2277-0011; Journal homepage: www.atbuftejoste.com

Parametrizing the time 't' into a vector of constant time periods

$$tym = \begin{vmatrix} t_i & t_1 & t_2 & \dots & t_c \\ t_c & t_1 & t_2 & \dots & t_f \end{vmatrix}^T, \text{then normalizing,} \quad (12)$$

$$tymN = tym/t_f \quad (13)$$

The orientation matrix of the end effector with time can be determined by applying the screw-symmetric axis formulation as follows;

$$|Q_{(e,\alpha)}| = \begin{vmatrix} e_x^2 cos'\alpha + cos\alpha & e_x e_y cos'\alpha - e_z sin\alpha & e_x e_z cos'\alpha + e_y sin\alpha \\ e_x e_y cos'\alpha + e_z sin\alpha & e_y^2 cos'\alpha + cos\alpha & e_y e_z cos'\alpha - e_x sin\alpha \\ e_x e_z cos'\alpha - e_y sin\alpha & e_y e_z cos'\alpha - e_x sin\alpha & e_z^2 cos'\alpha + cos\alpha \end{vmatrix} \quad (14)$$

Polynomials

Since the position and time at the beginning and end of every segment has been defined, and the orientation matrix is simplified to a single axis rotation, polynomials can be used to determine the robot end-effector's position and orientation at every time instant with reasonable computational efficiency. The cubic polynomial solution achieves a higher efficiency by trading off the ability to analyze acceleration while the quintic polynomial solution is capable of analyzing all variables (i.e. position, velocity, acceleration and time). A quintic polynomial requires the solution to the problem;

$$P = x_0 + x_1 * t + x_2 * t^2 + x_3 * t^3 + x_4 * t^4 + x_5 * t^5 \quad (15)$$

$$\dot{\theta} = x_1 + 2 * x_2 * t + 3 * x_3 * t^2 + 4 * x_4 * t^3 + 5 * x_5 * t^4 \quad (16)$$

$$\ddot{\theta} = 2 * x_2 + 6 * x_3 * t + 12 * x_4 * t^2 + 20 * x_5 * t^3 \quad (17)$$

This can be further simplified as follows;

$$\begin{vmatrix} P_i \\ \dot{\theta}_i \\ \ddot{\theta}_i \\ P_f \\ \dot{\theta}_f \\ \ddot{\theta}_f \end{vmatrix} = \begin{vmatrix} 1 & t_i & t_i^2 & t_i^3 & t_i^4 & t_i^5 \\ 0 & 1 & t_i & t_i^2 & t_i^3 & t_i^4 \\ 0 & 0 & 1 & t_i & t_i^2 & t_i^3 \\ 1 & t_f & t_f^2 & t_f^3 & t_f^4 & t_f^5 \\ 0 & 1 & t_f & t_f^2 & t_f^3 & t_f^4 \\ 0 & 0 & 1 & t_f & t_f^2 & t_f^3 \end{vmatrix} * \begin{vmatrix} x_0 \\ x_1 \\ x_2 \\ x_3 \\ x_4 \\ x_5 \end{vmatrix} \quad (18)$$

In the case of the cubic polynomial, the variables in the equations above can be reduced to satisfy the conditions for 3rd order solution. Inserting the values for position, velocity, acceleration and time the constants $|x_0\ x_1\ x_2\ x_3\ x_4\ x_5|^T$ can be determined. Substituting the values of the time vector 'tym' into the equation and using the newly determined constant vector 'x', the parametrized values for position/orientation angle (α), velocity and acceleration of the end-effector can be determined as it moves along the path. Observing that;

$$\alpha = |\alpha_i \quad \alpha_f| \quad (19)$$

(15)-(18) can be repeated for orientation angle by substituting Pi with α.

The change in orientation of the end-effector along the path can be determined by applying equation (14) above, keeping the unit vector constant and varying the parametrized orientation angle α as obtained in (19). The resultant transformation matrix would be;

$$T = \begin{vmatrix} Q_{(e,\alpha)} & P \\ 0 \quad 0 \quad 0 & 1 \end{vmatrix} \quad (20)$$

Applying the required inverse kinematic equations on the transformation matrix can explicitly determine all the joint angles of the robot. The trajectory analysis is independent of robot configuration.

Dynamic Analysis

With all the joint angles explicitly defined, the angular velocity of revolute joints (or the linear velocity of prismatic joints) can be easily determined by differentiating the joint position with time. The Newton-Euler recursive formulation is then applied to determine the parameterized joint torque as follows;

If 'ω' is the angular velocity of a link of the robot, then starting from the base and assuming that angular velocity, angular acceleration and linear acceleration at the base is always zero (0);

$$\omega_{i+1}^{i+1} = R_i^{i+1}\, \omega_i^i + \dot{\theta}_{i+1}\, Z_{i+1}^{i+1} \quad (21)$$

Where 'R' is the rotation matrix of the 'i^{th}' frame with respect to the '$i^{th}+1$' frame, '$\dot{\theta}$' is the angular velocity of the link as determined above and 'Z' is the unit vector along the joint

Corresponding author: Zhanqun Shi, Wei Wang ✉ *z_shi@hebut.edu.cn ✉ Department of Mechanical Engineering, Hebei University of Technology, Tianjin - China.

axis ($i.e\ [0,0,1]^T$). While $i = 0, 1, 2, \ldots, n$ and ω_i^i at the base is zero.

Likewise, the angular acceleration '$\dot{\omega}$' is also determined as follows;

$$\dot{\omega}_{i+1}^{i+1} = R_i^{i+1}\,\dot{\omega}_i^i + R_i^{i+1}\,\omega_i^i \times \dot{\theta}_{i+1}\,Z_{i+1}^{i+1} + \ddot{\theta}_{i+1}\,Z_{i+1}^{i+1} \quad (22)$$

Where the symbol '×' represents the cross-product. The Linear acceleration of the link '$\dot{v}$' can also be determined as follows;

$$\dot{v}_{i+1}^{i+1} = R_i^{i+1}\left(\dot{\omega}_i^i \times P_{i+1}^i + \omega_i^i \times \left(\omega_i^i \times P_{i+1}^i\right) + \dot{v}_i^i\right) \quad (23)$$

Where 'P' represents the position of the link. Gravitational effect acting on the manipulator can easily be accounted for by making the Linear velocity at the base a vector of gravity (i.e. $\dot{v}_i^i$ = | 0, g, 0 |^T instead of zeros as earlier stated). Then the Linear acceleration of the center of mass '$\dot{v}c$';

$$\dot{v}c_{i+1}^{i+1} = \dot{\omega}_{i+1}^{i+1} \times Pc_{i+1}^{i+1} + \omega_{i+1}^{i+1} \times \left(\omega_{i+1}^{i+1} \times Pc_{i+1}^{i+1}\right) + \dot{v}_{i+1}^{i+1} \quad (24)$$

'Pc' represents the position of the link at the centroid. Let 'Ic' represent the Moment of Inertia of the Link at the centroid, then the force 'F' and the torque 'N' acting on each link is determined as follows;

$$F_{i+1}^{i+1} = m_{i+1}\,\dot{v}c_{i+1}^{i+1} \quad (25)$$

$$N_{i+1}^{i+1} = Ic_{i+1}^{i+1}\,\dot{\omega}_{i+1}^{i+1} + \omega_{i+1}^{i+1} \times Ic_{i+1}^{i+1}\,\omega_{i+1}^{i+1} \quad (26)$$

The torque 'τ' acting on the joints can be determined from the resultant forces 'f' and torque 'n' acting on each link as a result of the surrounding links. Assuming that 'f' and 'n' acting on the End-Effector of the robot is zero (0), then starting from the n^{th} link, the joint torque can be determined with respect to the joints as follows;

$$f_i^i = R_{i+1}^i\,f_{i+1}^{i+1} + F_i^i \quad (27)$$

$$n_i^i = N_i^i + R_{i+1}^i\,n_{i+1}^{i+1} + Pc_i^i \times F_i^i + P_{i+1}^i \times R_{i+1}^i\,f_{i+1}^{i+1} \quad (28)$$

$$Therefore\ \ \tau_i = n_i^{i^T} Z_i^i \quad (29)$$

This can further be simplified by expressing it in state-space as follows;

$$\tau = M(\theta)\omega + V(\theta, \omega) + G(\theta) \quad (30)$$

Where the mass matrix of the manipulator is M (θ) with an [n x n] dimension, V (θ, ω) is the [n x 1] vector of the centrifugal and Coriolis term, and G (θ) is the [n x 1] vector of gravity. Similarly, the energy and power in the system can be derived as follows;

$$E = \tau \times \theta \quad (31)$$

$$P = \tau \times \omega \quad (32)$$

SIMULATION AND RESULTS

The algorithm was first tested on a 3 DOF manipulator and the results were compared with the results obtained from ADAMS before implementing on the proposed manipulator.

The manipulator was required to move from an initial position [500, -500, and 500] to a final position [500, 500, and 500] as shown in Fig. 2 below, with a maximum velocity of 0.27m/s in 7.29 seconds. It is assumed that the torque exerted by a link on the preceding joint is at a maximum when the manipulator arm is fully outstretched. Limited by singularity, the manipulator is simulated with the closest to singular configuration to be able to analyses the maximum possible torque in the joints. The manipulator was first simulated at force-free conditions then the manipulator was loaded with a 5kg and 10kg exerting a maximum torque of 5N and 10N respectively on the end-effector of the manipulator. The Fig 3 compares the results obtained from proposed algorithm and ADAMS. The Fig. 4 shows the position of the manipulator end-effector in the Cartesian-space and of the six revolute joints (Joint-space) derived from the inverse kinematics. Fig. 5 and 6 shows the velocity and acceleration of the robot in the Cartesian and Joints spaces. Fig. 7 shows the dynamic and energy plots for the industrial manipulator with no load, while the Fig. 8 and 9 shows the dynamic and energy plots for the manipulator with 5kg and 10kg loads respectively.

The values for the maximum velocity, acceleration, torque and cumulative energy in the joints are shown in table 2 below.

Corresponding author: Zhanqun Shi, Wei Wang ✉ *z_shi@hebut.edu.cn ✉ Department of Mechanical Engineering, Hebei University of Technology, Tianjin - China.

JOURNAL OF SCIENCE TECHNOLOGY AND EDUCATION 9(2), JUNE, 2021
ISSN: 2277-0011; Journal homepage: www.atbuftejoste.com

Table 2: Result of the Dynamic Simulation

s/n	Vel. (Rad/s)	Acc. (Rad/s^2)	Torque (N.m)			Energy (J)		
			0kg	*5kg*	*10kg*	*0kg*	*5kg*	*10kg*
1	0.54	0.26	2.50	9.68	17.16	2.31	9.79	19.84
2	0.13	0.10	3.01	10.14	17.38	1.30	2,85	5.68
3	0.39	0.45	0.08	6.99	14.06	0.10	6.51	13.03
4	0.00	0.00	0,16	7.23	14.30	0.00	0.00	0.00
5	0.27	0.37	0.01	7.07	14.15	0.01	4.82	9.63
6	0.54	0.26	0.00	5.00	10.00	0.01	9.63	15.71

Observations

i. The velocity and acceleration of the joints were kept constant in all simulations while the torque and energy dissipated in the joints increased with load.

ii. From the Table 2, it can be observed that the torque acting on the sixth joint is equal to the total external torque acting on the manipulator.

iii. The torque acting on the first and second joints is observed to be considerably higher than the torque acting on the other joints especially at no-load conditions. This can be said to be because the first and second links are reasonably larger and heavier than the links closer to the end-effector, furthermore the torque acting on the joints of the former links is an accumulation of all the torques acting on joints of the later links as described in iterative Newton- Euler dynamic algorithm.

iv. The torque acting on the sixth joint is the lowest yet the energy exerted is observed to be amongst the highest. It can also be observed that the velocity of the sixth joint is also amongst the highest which suggests that it covers more distance than the other joints. Therefore, the high energy exerted on the joint is justified.

v. It can also be observed that there is torque generated in the fourth joint actuator but the velocity and the energy exerted in the joint remains zero. This means that although there is no motion in the joint, the joint actuator is required to generate some static-torque to equalize the external forces acting on the joint. Since there is no motion in the joint, then there is no work done and therefore no energy was exerted in the joint.

vi. In Fig 6(b), 7(b) and 8(b) it can be observed that there are some inconsistencies in the energy plots. This is as a result of zero values in the parameterized position which gave NAN (Not a Number) or INF (Infinity) results during differentiation operations. In real operation, this can be avoided by carefully selecting the time periods or segments Δt (see equation 12).

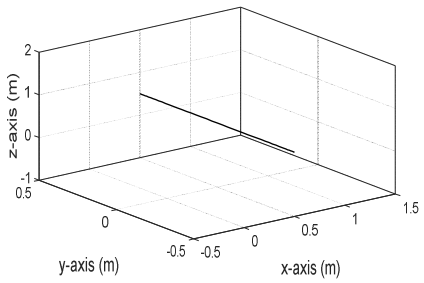

Figure 2. Motion Path of the End-Effector of an Industrial Manipulator in the Cartesian space.

*Corresponding author: Zhanqun Shi, Wei Wang ✉ *z_shi@hebut.edu.cn ✉ Department of Mechanical Engineering, Hebei University of Technology, Tianjin - China.*

CONCLUSIONS

In this paper an algorithm for analyzing the trajectory of an industrial manipulator was presented, a symbolic dynamic model was also developed based on Newton-Euler formulation. The trajectory algorithm parameterized the path of the manipulator in time which served as input variables for the dynamic model, describing the forces acting on every joint as it travels along the path. The result of the dynamic simulation presented herein was found to be more efficient than results obtained from ADAMS, and provides useful information for motor selection and design optimization of the manipulator. This allows students and researchers alike to design object specific manipulators and develop more efficient dynamic models capable of solving the problem of unstable oscillatory motion during operation of the manipulator thereby ensuring the maximum utility of the equipment.

RECOMMENDATIONS

It is obvious that if a special purpose manipulator is to be designed for light material transfer in an assembly line or other industrial applications requiring low loads (e.g. welding, flame cutting, etc.) and smaller motors would be required to power the joints of the manipulator especially towards the end-effector, whereas in applications like grinding, disc cutting, etc. where some reaction torque is generated which acts on the manipulator, larger motors would be required to power the joints. Generally industrial manipulators are built to be robust so as to finish most jobs in an industrial space. This may not be cost efficient as it neither optimizes the energy nor the performance of the robot manipulator.

*Corresponding author: Zhanqun Shi, Wei Wang ✉ *z_shi@hebut.edu.cn ✉ Department of Mechanical Engineering, Hebei University of Technology, Tianjin - China.*

JOURNAL OF SCIENCE TECHNOLOGY AND EDUCATION 9(2), JUNE, 2021
ISSN: 2277-0011; Journal homepage: www.atbuftejoste.com

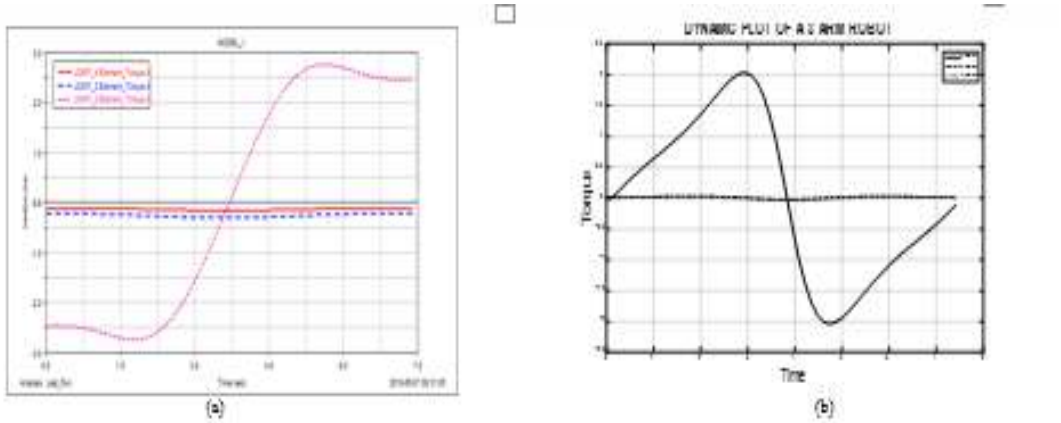

Figure 2. Dynamic plots of the Industrial Manipulator showing (a) Results obtaines from ADAMS (b) Results obtaines from proposed algorithm

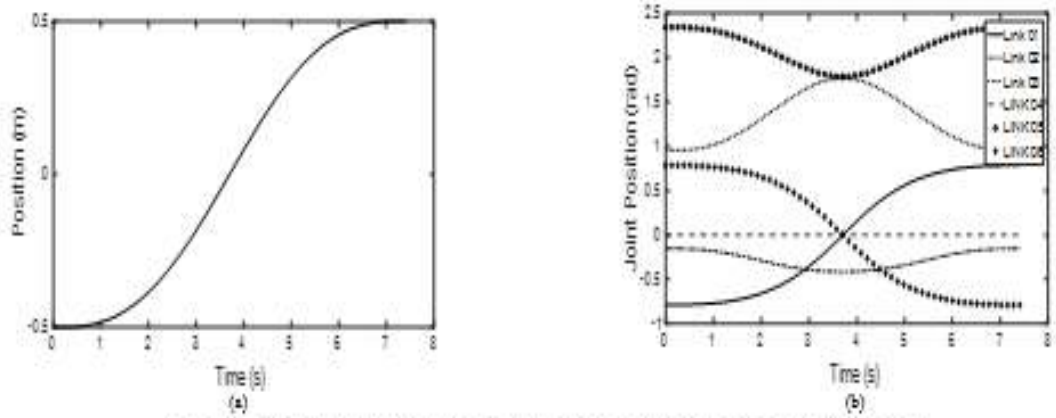

Figure 3. Position plots of the Industrial Manipulator in the (a) Cartesian space and (b) Joint space.

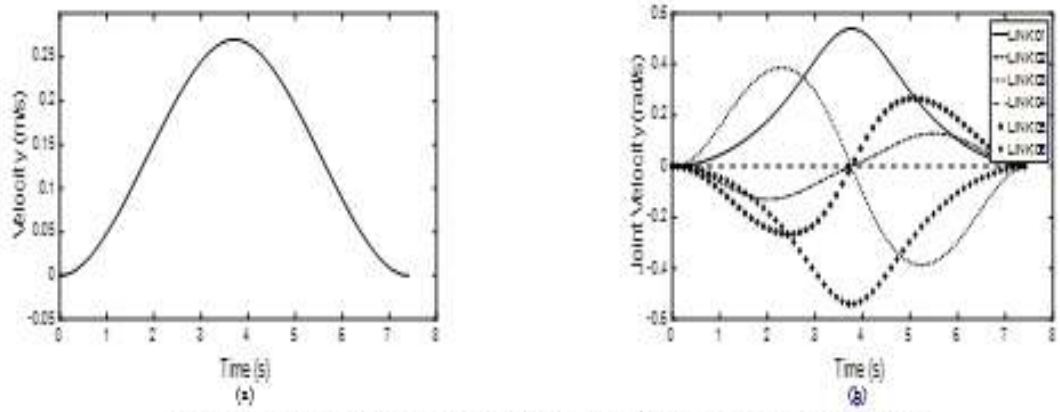

Figure 4. Velocity plots of the Industrial Manipulator in the (a) Cartesian space and (b) Joint space.

*Corresponding author: Zhanqun Shi, Wei Wang ✉ *z_shi@hebut.edu.cn ✉ Department of Mechanical Engineering, Hebei University of Technology, Tianjin - China.

JOURNAL OF SCIENCE TECHNOLOGY AND EDUCATION 9(2), JUNE, 2021
ISSN: 2277-0011; Journal homepage: www.atbuftejoste.com

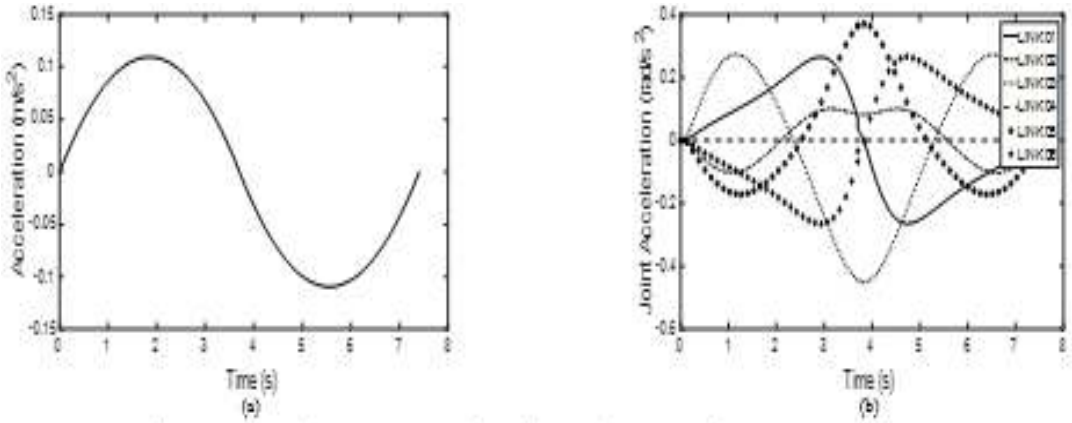

Figure 5. Acceleration plots of the Industrial Manipulator in the (a) Cartesian space and (b) Joint space.

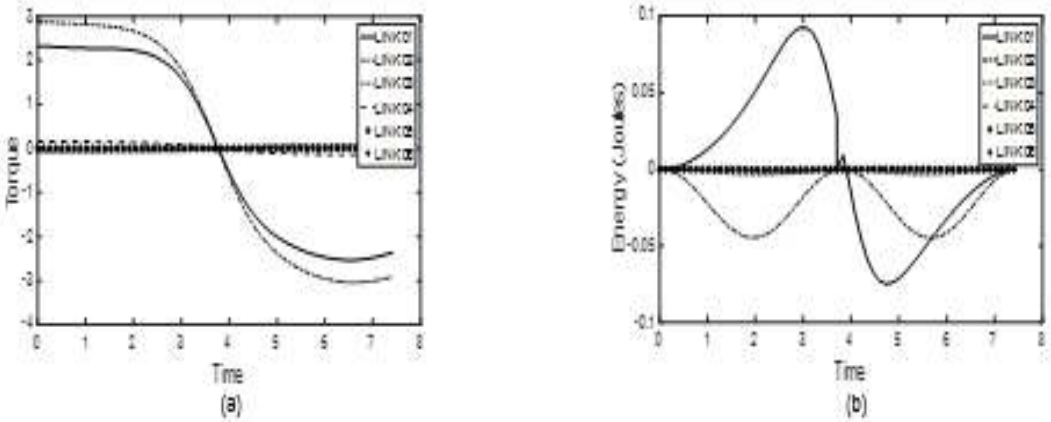

Figure 6. Dynamic plots of the Industrial Manipulator showing (a) Torque at 0kg load and (b) Energy at 0kg load.

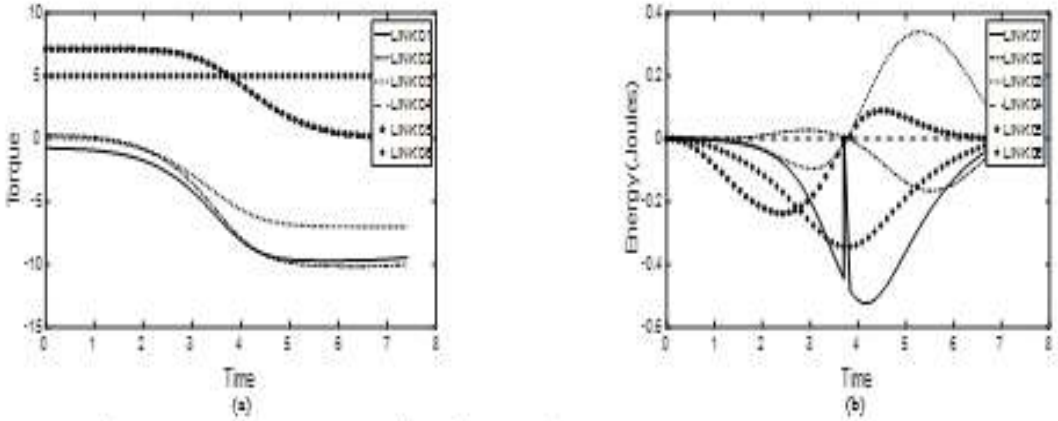

Figure 7. Dynamic plots of the Industrial Manipulator showing (a) Torque at 5kg load and (b) Energy at 5kg load.

*Corresponding author: Zhanqun Shi, Wei Wang ✉ *z_shi@hebut.edu.cn ✉ Department of Mechanical Engineering, Hebei University of Technology, Tianjin - China.

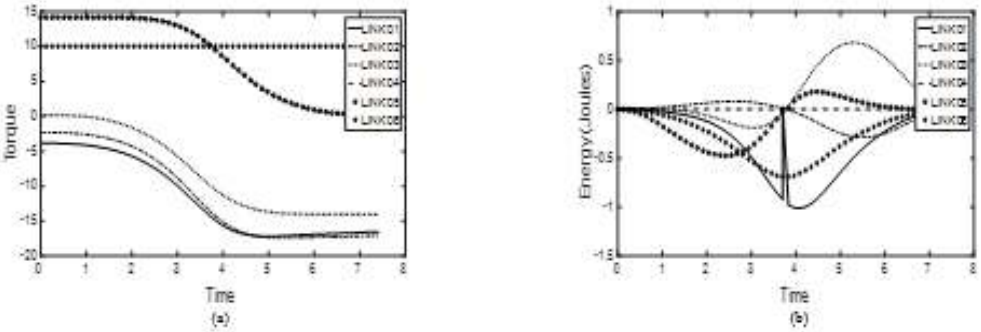

Figure 8. Dynamic plots of the Industrial Manipulator showing (a) Torque at 10kg load and (b) Energy at 10kg load.

REFERENCES

[1] Q.-H. Max Meng, "Comparison study of model-based and non-model-based robot controllers," 1995 IEEE Int. Conf. Syst. Man Cybern. Intell. Syst. 21st Century, vol. 1, pp. 61–66, 1995.

[2] S. Jiang et al., "A typical dynamic parameter identification method of 6-degree-of-freedom industrial robot," Proc. Inst. Mech. Eng. Part I J. Syst. Control Eng., vol. 231, no. 9, pp. 740–752, 2017.

[3] S K Saha, 'Introduction to Robotics', ISBN: 0-07-066900-7, McGraw-Hill Publishing Company Limited, 2008.

[4] Lung-Wen Tsai, 'Robot Analysis', ISBN-10: 0471325937, ISBN-13: 978-0471325932, Wiley-Interscience Publisher, 1999.

[5] Mark W Spong, M. Vidyasagar, "Robot Dynamics And Control", ISBN: 8126517808, 9788126517800, Wiley India Pvt. Limited, 2008.

[6] John J. Craig, "Introduction to Robotics", ISBN: 0-13-123629-6, Pearson Education, Inc. 2005

[7] B. Fardenesh and J. Rastega, "A New Model-Based Tracking Control foe Robot Manipulators Using Trajectory Pattern Inverse Dynamics", Short Papers - IEEE Trans. Robot. Automat. vol. 8, no. 2, pp. 279–285, 1992.

[8] H. Davis and W. Book, "Torque control of a redundantly actuated passive manipulator," in American Control Conference, Proceedings of the 1997, vol. 2, pp. 959–963, 1997.

[9] H. Cheng, Y.-K. Yiu, and Z. Li, "Dynamics and control of redundantly actuated parallel manipulators," IEEE/ASME Transactions on mechatronics, vol. 8, no. 4, pp. 483–491, 2003.

[10] C. Yang, G. Ganesh, S. Haddadin, S. Parusel, A. Albu-Schaeffer, and E. Burdet, "Human-like adaptation of force and impedance in stable and unstable interactions," IEEE transactions on robotics, vol. 27, no. 5, pp. 918–930, 2011.

[11] Pradeep K. Khosla and Takeo Ksnade, "Parameter Identification of Robot Dynamics" Proceedings of the IEEE Conference on Decision and Control, p 1754-1760, 1985

[12] Z.-H. Jiang and H. Senda, "Dynamic parameter identification of robot arms with servo-controlled electrical motors," vol. 6042, p. 604235, 2005

[13] W. Wu, S. Zhu, X. Wang, and H. Liu, "Closed-loop dynamic parameter identification of robot manipulators using modified fourier series," Int. J. Adv. Robot. Syst., vol. 9, 2012

[14] M. Gautier and S. Briot, "Dynamic parameter identification of a 6 DOF industrial robot using power model," 2013 IEEE Int. Conf. Robot. Autom., pp. 2914–2920, 2013

[15] C. Yang, Y. Jiang, W. He, J. Na, Z. Li, and B. Xu, "Adaptive Parameter Estimation and Control Design for Robot Manipulators with Finite-Time Convergence," IEEE Trans. Ind. Electron., vol. 0046, no. c, 2018

[16] C. Liu, "Kinematical and Dynamic Analysis of 6-DOF Industrial Robot," 2016 9th International Symposium on Computational Intelligence and Design (ISCID), Hangzhou, pp. 32-35, 2016.

[17] D. I. Park, C. Park, H. Do, T. Choi and J. Kyung, "Design and analysis of dual arm robot using dynamic simulation," 2013 10th International Conference on Ubiquitous Robots and Ambient Intelligence (URAI), Jeju, pp. 681-682, 2013.

[18] V. D. Tourassis, "Principles and design of model-based robot controllers," Int. J. Control, vol. 47, no. 5, pp. 1267–1275, 1988

[19] J. Y. S. Luh, M. W. Walker. and R. P. Paul, "On-line computational scheme for mechanical manipulators," Journal of Dynamic Systems, measurement and Control, vol. 102, no. 2, pp. 69-76, June 1980

[20] John J Murray, Charles P Neuman, "Organizing Customized Robot Dynamics Algorithms for Efficient Numerical Evaluation," IEEE Transactions on Systems, Man, and Cybernetics, vol. 18, no. 1, 1988. P115 – 126

*Corresponding author: Zhanqun Shi, Wei Wang ✉ *z_shi@hebut.edu.cn ✉ Department of Mechanical Engineering, Hebei University of Technology, Tianjin - China.